

Supporting Information

Localized Surface Plasmon Resonance Effect Enhanced Cu/TiO₂ Core-Shell Catalyst for boosting CO₂ Hydrogenation Reaction

Lizi Shi ^a, Huimin Liu ^{b*}, Shangbo Ning ^a and Jinhua Ye ^{a, c*}

a. TJU-NIMS International Collaboration Laboratory, School of Materials Science and Engineering, Tianjin University, Tianjin 300072, P. R. China

b. School of Chemical and Environmental Engineering, Liaoning University of Technology, Jinzhou 121001, China.

c. International Center for Materials Nanoarchitectonics (WPI-MANA), National Institutes for Materials Science (NIMS), 1-1 Namiki, Tsukuba, Ibaraki 305-0044, Japan

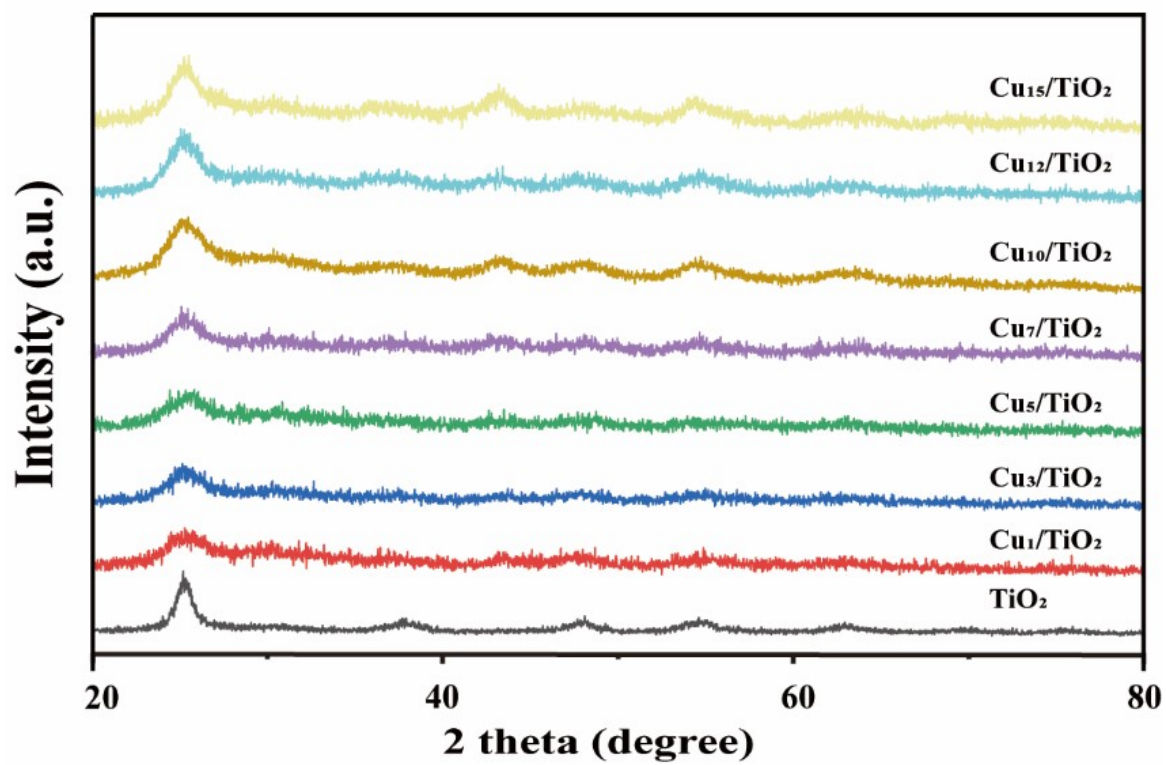


Figure S1. XRD patterns of photo-reduced Cu_x/TiO_2 ($x=1, 3, 5, 7, 10, 12, 15$).

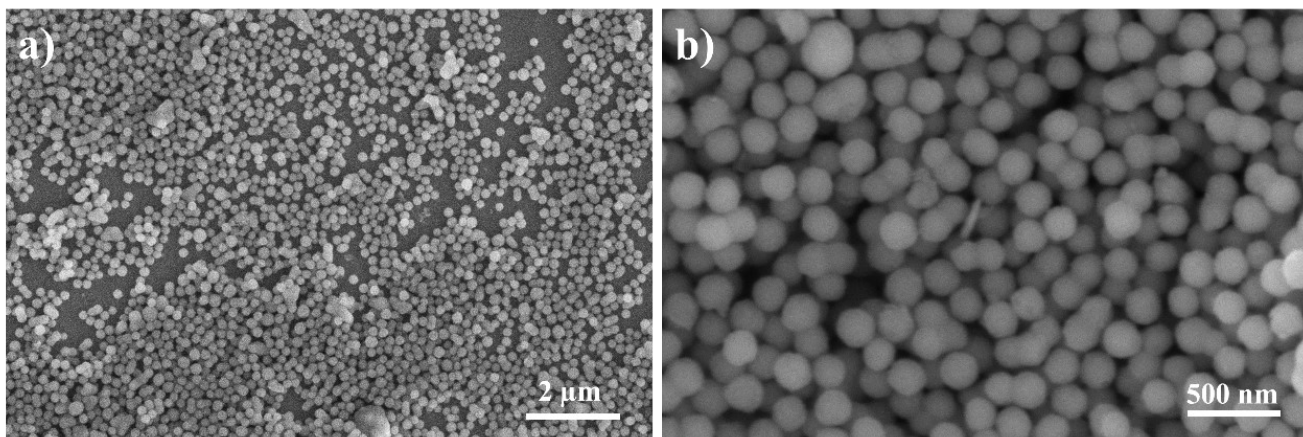


Figure S2. SEM images of SiO₂ nanoparticles: (a) large scale and (b) local distribution.

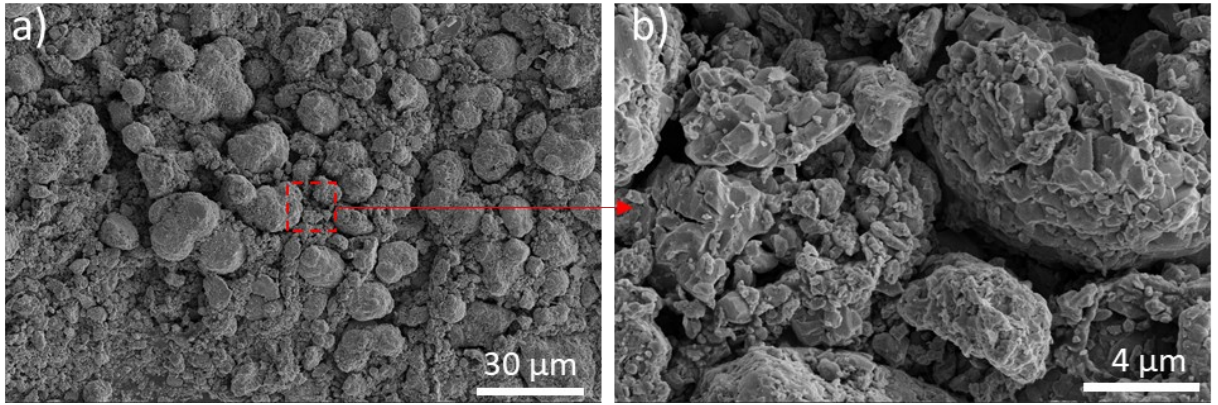


Figure S3. SEM images of Cu after calcining at 700 °C for 2h. Cu was severe sintered at high temperature (700°C)

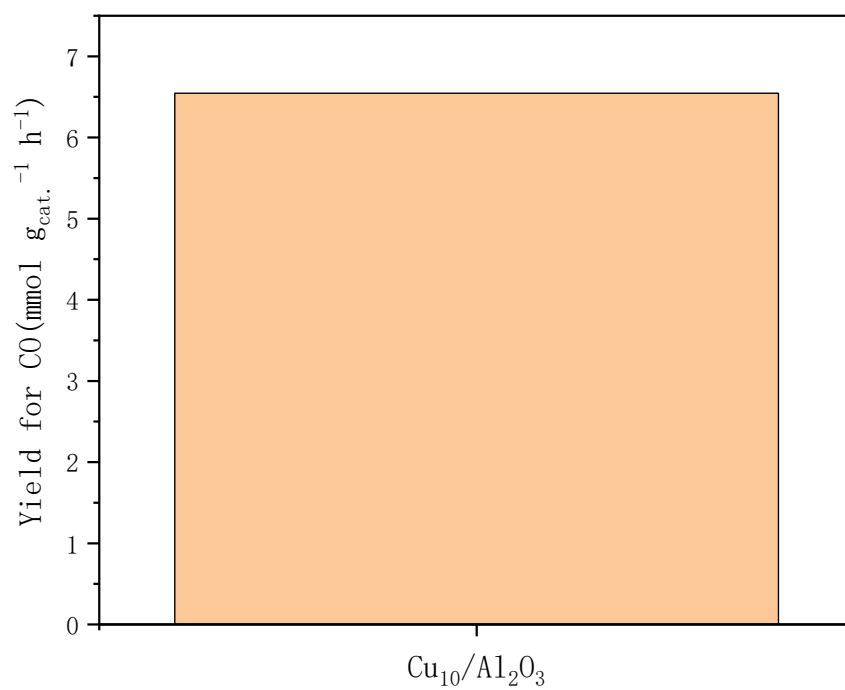


Figure S4. CO yield on Al₂O₃ under light illumination.

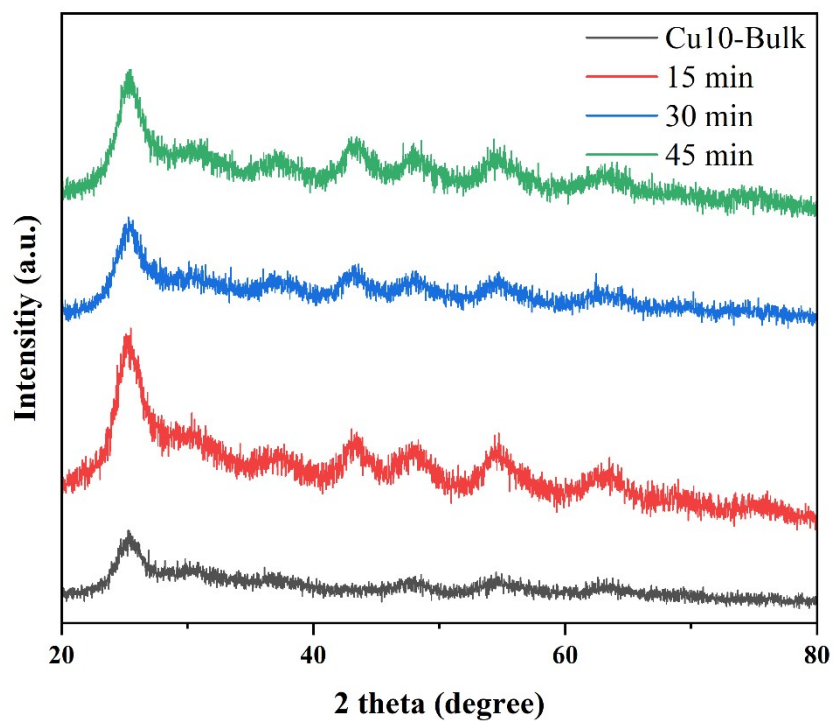


Figure S5. XRD patterns of Cu₁₀/TiO₂ for before photoreduction (Cu10-Bulk) and different photoreduction time (10~45 min).

Table S1. BET surface areas of different samples.

| Sample | Cu ₁₀ /TiO ₂ Rutile | Cu/P25 | Cu ₁₀ /TiO ₂ Before Reduction | Cu/ Al ₂ O ₃ |
|---|--|--------|---|------------------------------------|
| BET surface area (m ² /g) | 10.113 | 26.155 | 73.937 | 147.688 |
| Pore diameter (nm) | 3.706 | 64.632 | 3.940 | 5.797 |

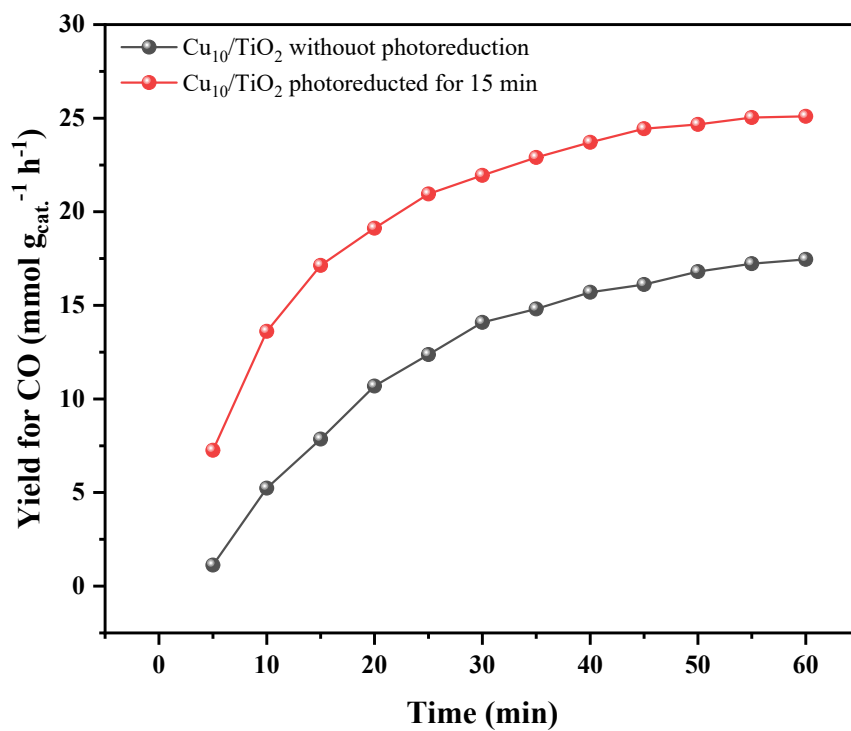


Figure S6. CO yield of Cu₁₀/TiO₂ catalyst under different treatment: without photoreduction and photo-reduced for 15 min.

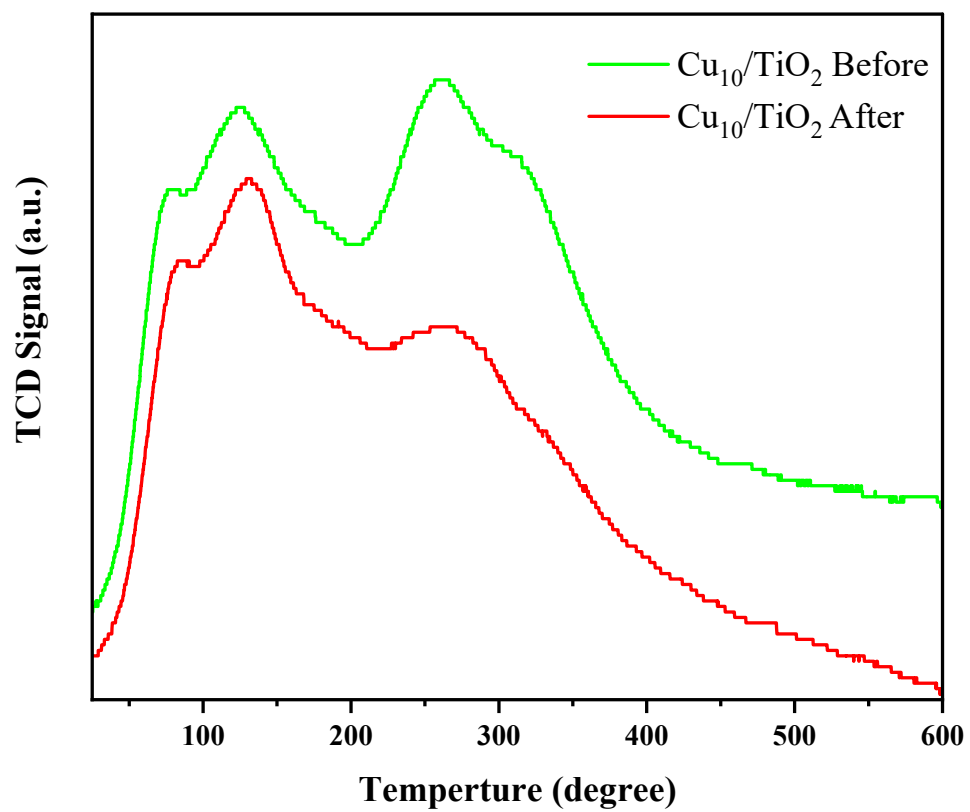


Figure S7. TPD CO₂ desorption profiles for Cu₁₀/TiO₂ before and after photoreduction.

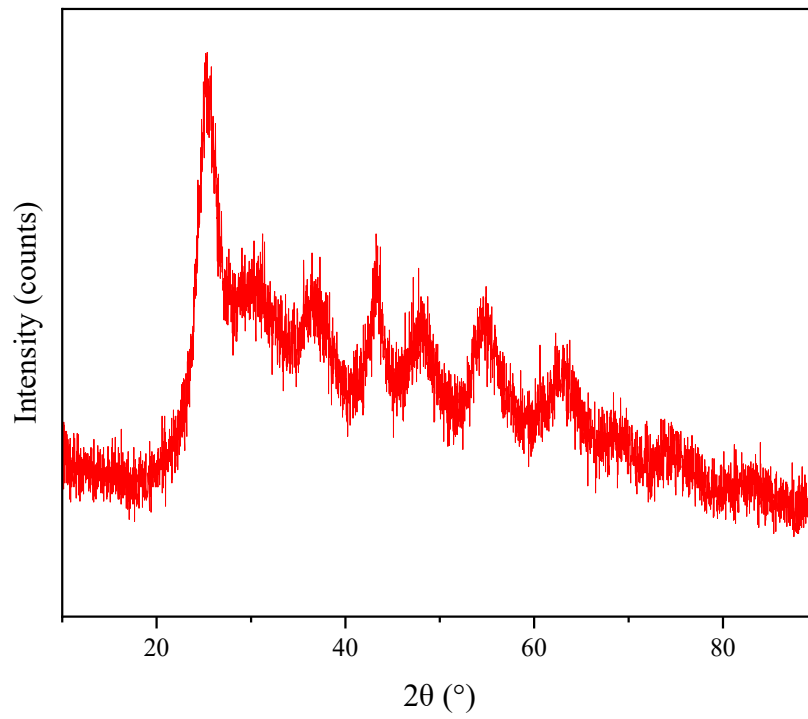


Figure S8. XRD patterns of $\text{Cu}_{10}/\text{TiO}_2$ after reduction at 10% H_2/Ar atmosphere 450 °C for 2 hours.

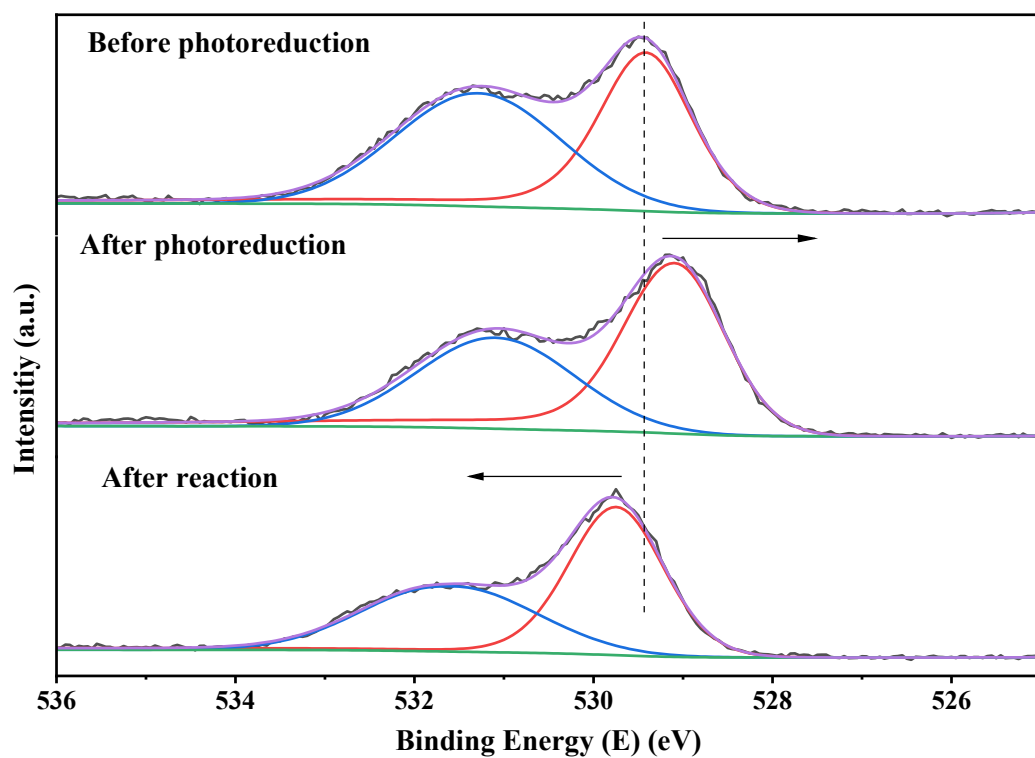


Figure S9. High resolution XPS image of O element at different sample condition ($\text{Cu}_{10}/\text{TiO}_2$, before photoreduction, after photoreduction and after reaction).

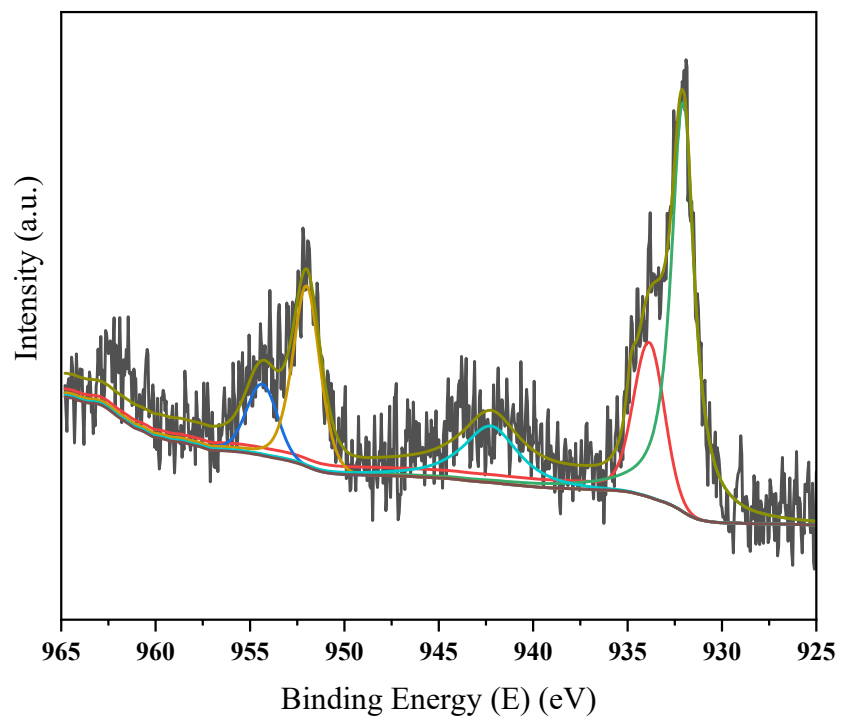


Figure S10. Cu 2p high resolution XPS spectra of Cu₁₀/TiO₂.

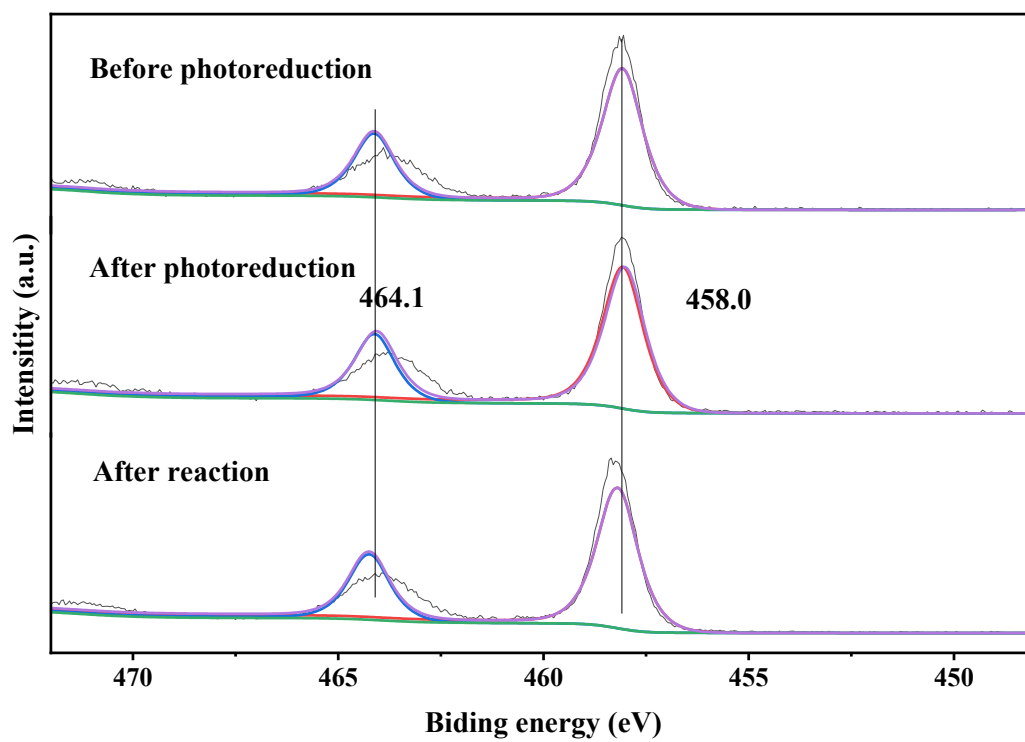


Figure S12. Comparison of chemical state of Ti element in different conditions ($\text{Cu}_{10}/\text{TiO}_2$, before photoreduction, after photoreduction and after reaction).

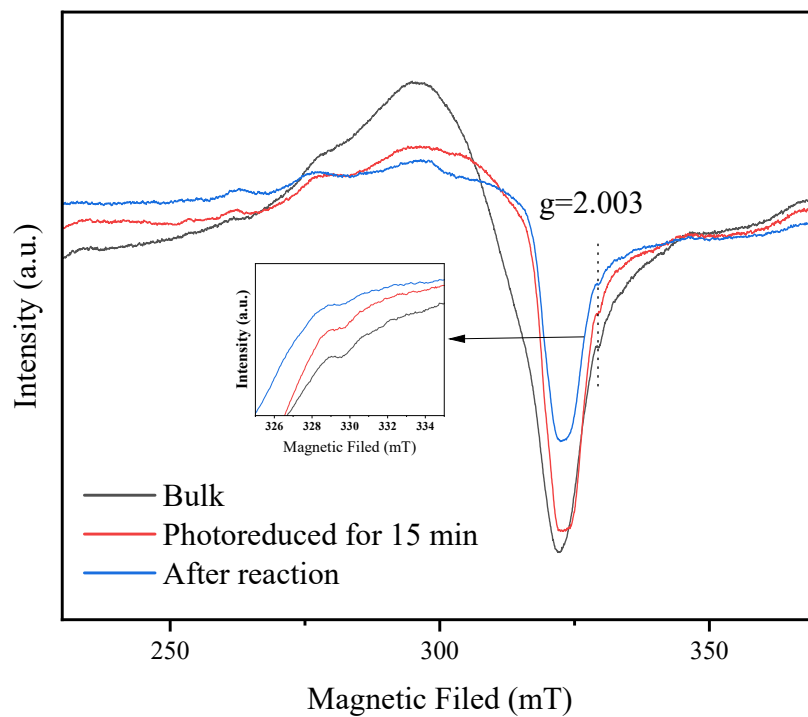


Figure S13. X-Band EPR spectra for $\text{Cu}_{10}/\text{TiO}_2$ under different conditions. “Bulk” means that $\text{Cu}_{10}/\text{TiO}_2$ was used for test without any reduction, neither photoreduction nor thermal reduction at H_2/Ar atmosphere.

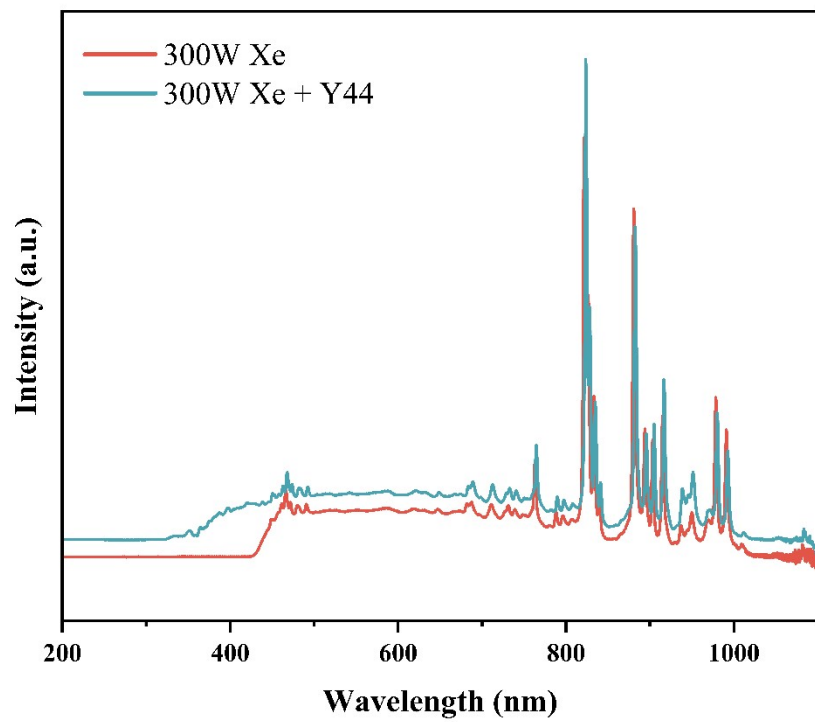


Figure S14. Spectrum of 300W Xe lamp without any filter and with Y44 filter.

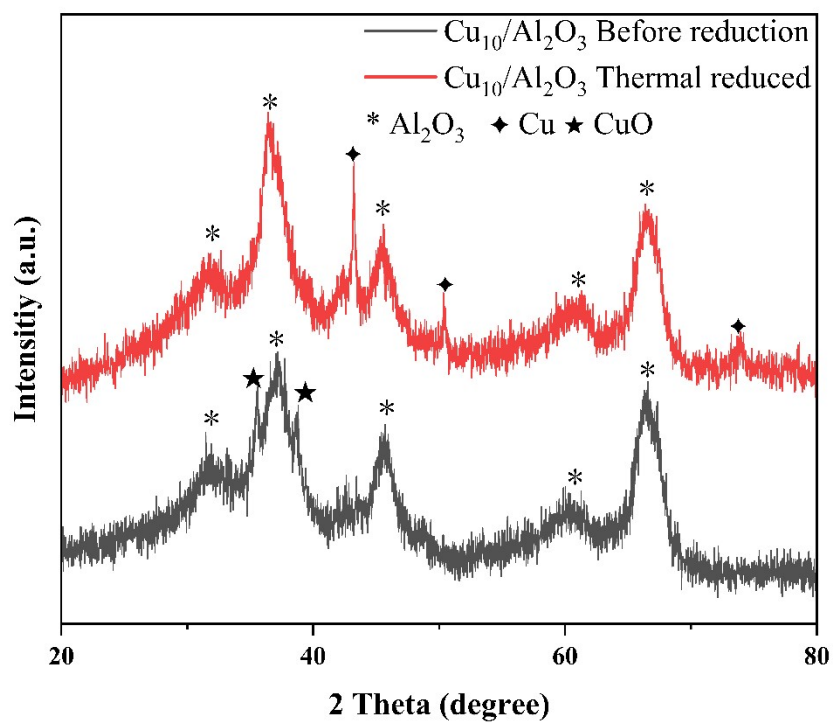


Figure S15. XRD patterns of Cu₁₀/Al₂O₃ before and after thermal reduction. Thermal reduction was taken place in a H₂/Ar atmosphere for two hours at 450 °C.

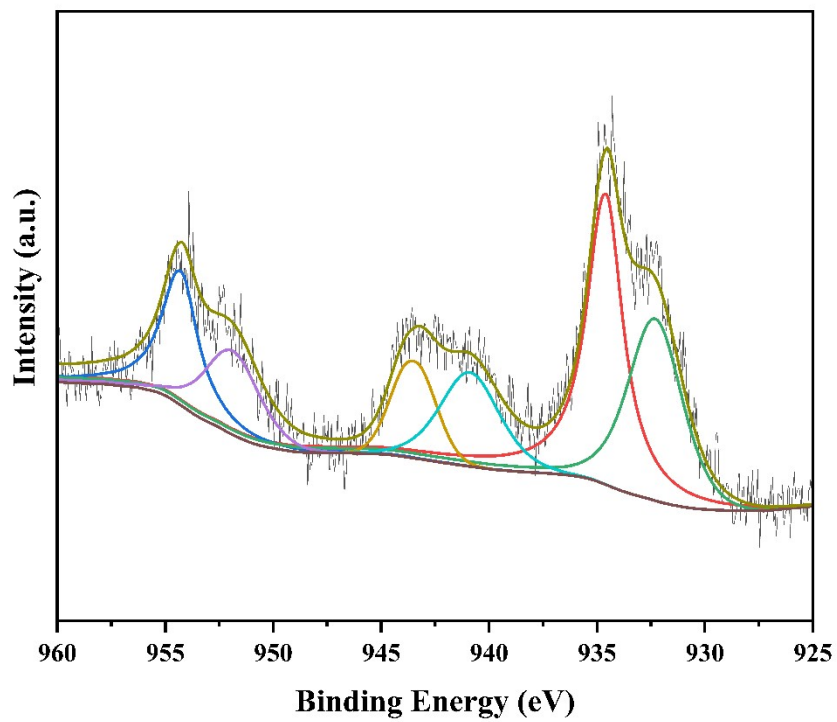


Figure S16. Cu 2p high resolution XPS spectra of Cu₁₀/Al₂O₃ after thermal reduction. Thermal reduction was taken place in a H₂/Ar atmosphere for two hours at 450 °C. Cu (II) is primarily formed as a result of oxidation while waiting for the test.

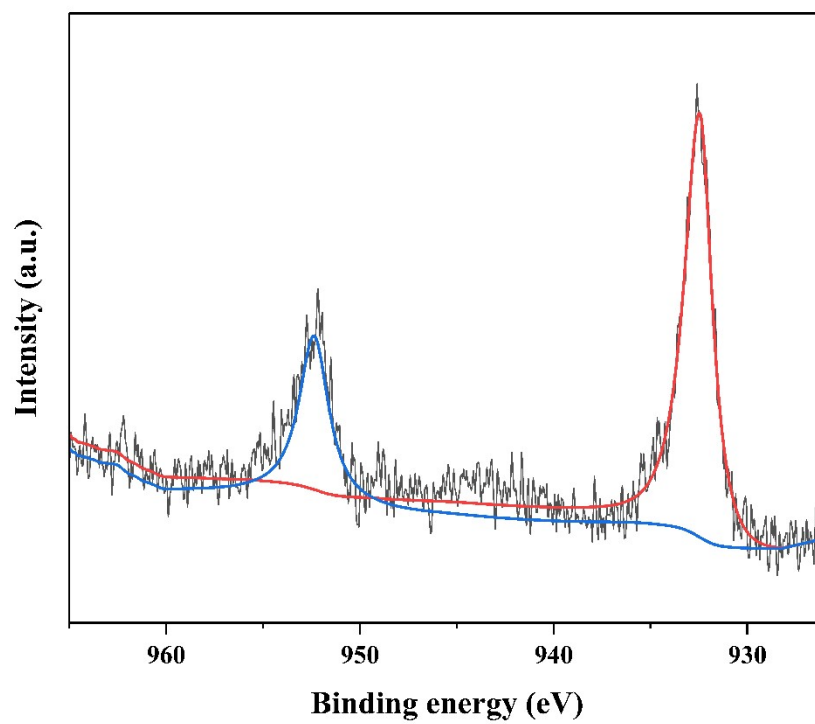


Figure S17. Cu 2p high resolution XPS spectra of $\text{Cu}_{10}/\text{TiO}_2$ after thermal reduction. Thermal reduction was taken place in a H_2/Ar atmosphere for two hours at 450 °C.

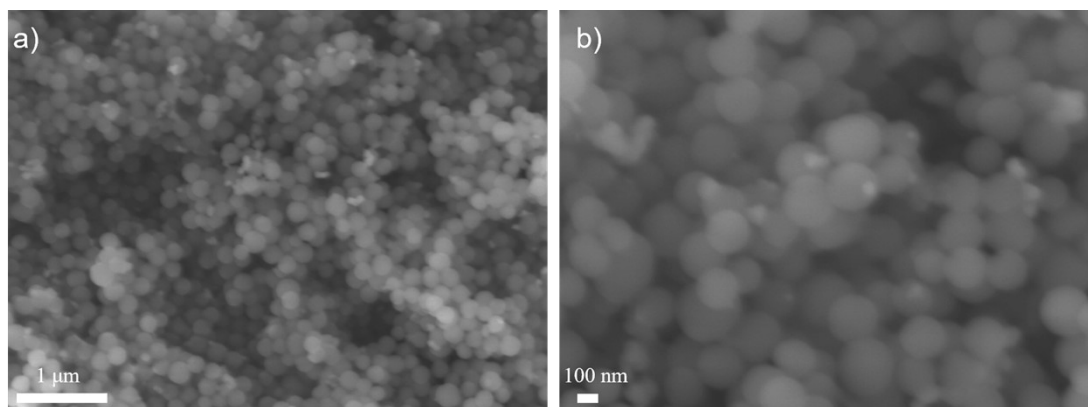


Figure S18. SEM images of Cu₁₀/TiO₂ after reaction. (a) Large scale, 1 μm; (a) Local scale, 100 nm. The bright spots in the picture are suspected to be aggregated Cu (0).

Table S2. Catalyst activity under different reduction time and reduction ways: photo-reduced varies from 0 to 45 min and reduced at 10% H₂/Ar atmosphere 450 °C for 2 hours.

| Reduction Parameters | Photo-reduced for 0 min | Photo-reduced for 5 min | Photo-reduced for 10 min | Photo-reduced for 15 min | Photo-reduced for 30 min | Photo-reduced for 45 min | Reduction with H ₂ /Ar at 450 °C for 2h |
|--|-------------------------|-------------------------|--------------------------|--------------------------|--------------------------|--------------------------|--|
| CO yield (mmol g ⁻¹ h ⁻¹) | 17.453 | 10.007 | 19.631 | 25.100 | 19.778 | 22.247 | 23.06 |

Table S3. Recent works relevant to photothermal CO₂ hydrogenation reactions.

| Catalyst | Type of Reactor | Light Source | Temperature (°C) | CO ₂ :H ₂ Ratio | Yield of CO (mmol g ⁻¹ h ⁻¹) | Yield of CH ₄ (mmol g ⁻¹ h ⁻¹) | Selectivity of CO ₂ (%) | Year | Reference |
|--|-----------------|---|------------------|---------------------------------------|---|--|------------------------------------|------|-----------|
| Ni/TiO ₂ - _x H _x | Flow | 300 W Xe lamp | 441.2 | 1:1 | ~1.0 | ~2.7 | / | 2022 | 1 |
| FeCe-300 ^a | Flow | 300 W Xe lamp, (2.2 W cm ⁻²) | 450 | 1:4 | 19.61 | Trace | ~100 | 2020 | 2 |
| Ni-600 ^b | Flow | 300 W Xe lamp | ~260 | 1:4 | Trace | 278.8 | ~0 | 2021 | 3 |
| Fe ₃ O ₄ | Flow | 300 W Xe lamp, (2.05 W cm ⁻²) | ~350 | 1:2 | 11.3 | Trace | ~100 | 2020 | 4 |
| Ni/SiO ₂ ·Al ₂ O ₃ | Batch | 300 W Xe lamp, (1.3 W cm ⁻²) | 113.7 | 1:1 | 4.53 | 11.6 | / | 2020 | 5 |
| CsPbBr ₃ @CsPb ₂ Br ₅ | Batch | 300 W Xe lamp, (220 mW cm ⁻²) | 200 | 1:3 | 0.069 | / | / | 2022 | 6 |
| In ₂ O _{3-x} | Batch | 300 W Xe lamp | 262 | 1:1 | 2.38 | ~0 | ~100 | 2020 | 7 |
| Ni-BTO | Batch | 300 W Xe lamp, (293 mW cm ⁻²) | / | 1:4 | Trace | 257 | 3.6 | 2021 | 8 |
| RuO ₂ /STO | Batch | 300 W Xe lamp, (108 mW cm ⁻²) | 150 | 1:4 | / | 14.6 | / | 2019 | 9 |
| Ru-Al ₂ O _{3-x} -L | Batch | 300 W Xe lamp | 236.4 | 1:4 | / | 14.04 | / | 2022 | 10 |
| Pt/H _x MoWO _y | Flow | 500W Hg-Xe short arc lamp, λ>450nm | 140 | 1:1 | 3.1 | Trace | ~100 | 2022 | 11 |
| 0.35Ru@NVO | Batch | 300 W Xe lamp, (2.0 W cm ⁻²) | 350 | 1:4 | / | 114.9 | 5 | 2021 | 12 |
| Ni@C-600 ^c | Flow | 300 W Xe lamp, (4.3 W cm ⁻²) | 272 | 1:4 | / | 154 | 2.3 | 2021 | 13 |
| Ni/N _{5.0} -CeO ₂ | Batch | 300 W Xe lamp, (2.11 W | 350 | 1:1 | 20.9 | Trace | ~100 | 2021 | 14 |

| | | | | | | | | | |
|---------------------------------------|-------|--|------|-----|------|-------|------|------|-----------|
| ASA-c-Ag ₈ Cu ₁ | Batch | cm ⁻² 300 W Xe lamp, (3.7 W cm ⁻²) | >300 | 1:1 | 5.4 | 19.9 | / | 2022 | 15 |
| Cu ₁₀ /TiO ₂ | Batch | 300 W Xe lamp, (2.4 W cm ⁻²) | 334 | 1:1 | 25.1 | Trace | ~100 | / | This Work |

- An FeCe-300 catalyst with an Fe:Ce molar ratio of 2:1, The final products are denoted as FeCe-x, where x refers to the reduction temperature. For the FeCe-300 catalysts, the Fe: Ce molar
- The number '600' means the Ni-based catalysts (Ni-x) have been prepared by reducing NiAl-LDH nanosheets precursor at 600 °C
- The precursor was placed in the reactor under continuous flow of N₂ followed by direct carbonization at 600 °C for 6 h under N₂ (25 mL min⁻¹) using a heating ramp of 2 °C min⁻¹. After cooling down of the reactor the samples were passivated in continuous flow of N₂ (25 mL min⁻¹) and Air (5 mL min⁻¹) for 2 hours.

Note: “/” means that the author did not provide relevant information in their article.

References

- 1 Y. Li, Z. Zeng, Y. Zhang, Y. Chen, W. Wang, X. Xu, M. Du, Z. Li and Z. Zou, *ACS Sustainable Chemistry and Engineering*, , DOI:10.1021/ACSSUSCHEMENG.2C01081/ASSET/IMAGES/LARGE/SC2C01081_0004.JPEG.
- 2 J. Zhao, Q. Yang, R. Shi, G. I. N. Waterhouse, X. Zhang, L. Z. Wu, C. H. Tung and T. Zhang, *NPG Asia Materials*, , DOI:10.1038/s41427-019-0171-5.
- 3 Z. Li, R. Shi, J. Zhao and T. Zhang, *Nano Research* 2021 14:12, 2021, **14**, 4828–4832.
- 4 C. Song, X. Liu, M. Xu, D. Masi, Y. Wang, Y. Deng, M. Zhang, X. Qin, K. Feng, J. Yan, J. Leng, Z. Wang, Y. Xu, B. Yan, S. Jin, D. Xu, Z. Yin, D. Xiao and D. Ma, *ACS Catalysis*, 2020, **10**, 10364–10374.
- 5 M. J. Cai, C. R. Li and L. He, *Rare Metals*, 2020, **39**, 881–886.
- 6 P. Gao, Z. Cui, X. Liu, Y. Wu, Q. Zhang, Z. Wang, Z. Zheng, H. Cheng, Y. Liu, Q. Li, B. Huang and P. Wang, *Chemistry – A European Journal*, 2022, e202201095.
- 7 L. Wang, Y. Dong, T. Yan, Z. Hu, A. A. Jelle, D. M. Meira, P. N. Duchesne, J. Y. Y. Loh, C. Qiu, E. E. Storey, Y. Xu, W. Sun, M. Ghossoub, N. P. Kherani, A. S. Helmy and G. A. Ozin, *Nature Communications* 2020 11:1, 2020, **11**, 1–8.
- 8 D. Mateo, N. Morlanes, P. Maity, G. Shterk, O. F. Mohammed, J. Gascon, D. Mateo, N. Morlanes, G. Shterk, J. Gascon, P. Maity and O. F. Mohammed, *Advanced Functional Materials*, 2021, **31**, 2008244.
- 9 D. Mateo, J. Albero and H. García, *Joule*, 2019, **3**, 1949–1962.
- 10 X. Liu, C. Xing, F. Yang, Z. Liu, Y. Wang, T. Dong, L. Zhao, H. Liu and W. Zhou, *Advanced Energy Materials*, 2022, **2201009**, 2201009.
- 11 H. Ge, Y. Kuwahara, K. Kusu, H. Kobayashi and H. Yamashita, *Journal of Materials Chemistry A*, 2022, **10**, 10854–10864.
- 12 Y. Chen, Y. Zhang, G. Fan, L. Song, G. Jia, H. Huang, S. Ouyang, J. Ye, Z. Li and Z. Zou, *Joule*, 2021, **5**, 3235–3251.
- 13 I. S. Khan, D. Mateo, G. Shterk, T. Shoinkhorova, D. Poloneeva, L. Garzón-Tovar and J. Gascon, *Angewandte Chemie International Edition*, 2021, **60**, 26476–26482.
- 14 Z. Jia, S. Ning, Y. Tong, X. Chen, H. Hu, L. Liu, J. Ye and D. Wang, *ACS Applied Nano Materials*, 2021, **4**, 10485–10494.
- 15 T. Shao, X. Wang, H. Dong, S. Liu, D. Duan, Y. Li, P. Song, H. Jiang, Z. Hou, C. Gao, Y. Xiong, T. Shao, X. Wang, H. Dong, S. Liu, D. Duan, Y. Li, H. Jiang, Z. Hou, C. Gao and Y. Xiong, *Advanced Materials*, 2022, **34**, 2202367.